

# On the Performance of Cellular Networks with Adaptive Modulation and Energy Harvesting—A Stochastic Geometry Approach

Nhut-Minh Ho

Post and Telecommunications Institute of Technology  
Ho Chi Minh City, Vietnam  
minhho@ptithcm.edu.vn

Sang Quang Nguyen (\*)

Ho Chi Minh City University of Transport  
Ho Chi Minh City, Vietnam  
sang.nguyen@ut.edu.vn  
(\*) Corresponding author

Thanh-Toan Phan

Post and Telecommunications Institute of Technology  
Ho Chi Minh City, Vietnam  
phanthanhtoan@ptithcm.edu.vn

Lam-Thanh Tu

Ton Duc Thang University  
Ho Chi Minh City, Vietnam  
tulamthanh@tdtu.edu.vn

**Abstract**—The performance of ultra-dense cellular networks considering both adaptive discrete modulation (ADM) and energy harvesting (EH) is investigated. Particularly, mobile users (MUs) are charged its battery from all ambient radio frequency (RF) signals. Based on the amount of harvested energy as well as the channel conditions, MU will actively choose an appropriate modulation scheme that not only maximizes the rate but also satisfies the quality-of-service (QoS). Moreover, we consider the spatial-temporal correlation at the signal-to-interference-plus-noise ratios (SINRs) of base stations (BSs) which are totally different from work in the literature. Several important metrics are investigated such as, occurrence probabilities of different modulation schemes (Poc), coverage probability (Pcov), and achievable spectral efficiency (ASE). Finally, the results highlight the superiority of the proposed scheme compared to the conventional fixed modulation.

**Index Terms**—Adaptive Modulation, Energy Harvesting, Performance Analysis, Stochastic Geometry

## I. INTRODUCTION

With the growing in the number of wirelessly connected devices, the demand for the power to feed such ultra-dense networks has attracted researchers [1]. Moreover, another issue of the ultra-dense networks is how to increase the spectral efficiency (SE) since the network is in the interference-limited regime rather than the noise-limited or neither of them. To overcome these unavoidable issues in the ultra-dense networks some advanced technologies are employed in the literature, for example, the cognitive radio networks (CRNs) [2], [3] that is proved to be an effective way to improve the SE, the satellite communications that can provide service at every corner of the earth without creating interference at the terrestrial [4], the interference alignment technique that takes the advantages of the multiple antennae at both transmitter and receiver to suppress the interference [5] and the adaptive discrete modulation (ADM) that significantly scales up the

average rate thus improving the SE [6]. Particularly, a properly modulation scheme is chosen at the transmitter relying on the practical channel conditions to maximize the average rate thus facilitating the ASE. Nonetheless, these above techniques generally improve the SE of the wireless networks while the enhancement of energy efficiency (EE) is minor compared with the SE. Fortunately, another advanced technique called energy harvesting (EH) [7] has recently attracted many researchers since it allows the low energy devices (LEDs) to harvest energy from the surrounding radio frequency (RF) thus providing a solid response to the question *How to feed an ultra-dense network*. As a consequence, in the present work, we explore the performance of the ultra-dense cellular network by considering both ADM and EH techniques. Before going to discuss the novelties as well as the contributions of the considered networks, state-of-the-art of ADM, EH, and other advanced techniques are first visited.

### A. State-of-the-art

The performance of the key metrics in modern wireless networks such as outage probability (OP), coverage probability (Pcov), ergodic capacity, spectral efficiency, and energy efficiency was studied extensively in [8]–[16]. The cooperative unmanned aerial vehicles (UAV) non-orthogonal multiple access (NOMA)-based in short packet communications (SPC) was studied in [8]. Particularly, the average end-to-end (e2e) block-error rates (BLERs) were derived in the closed-form expression. A novel expression of closed-form of the Pcov in the long-range (LoRa) networks was given in [9]. A tractable framework of both Pcov and ergodic capacity in cellular networks based on tools from stochastic geometry (SG) was derived by Andrews and other authors in [10]. Meanwhile, the closed-form expression of ergodic capacity in multi-hop decode and forward (DF) was given in [11].

Duy and others in [12] derived outage probability expressions in cognitive radio networks. Moreover, the transmit power of the secondary transmitter was computed in [13]. On the other hand, the performance of the combination of optical communications and wireless communications was conducted in [14] where RF signals are seamlessly transmitted through both fiber and mmWave. The impact of hardware impairment in UAV-NOMA-based systems was investigated in [15]. Their outcomes showed that the performance of the near user outperforms its counterpart under the influences of hardware impairments. A recently proposed definition of the Pcov that takes into account the correlation of the signal-to-interference ratios (SIRs) and signal-to-noise ratios (SNRs) at end-devices of the LoRa was comprehensively studied [16]. They also point out the influences of density of EDs on the performance of the coverage probability and spectral efficiency under different transmit power regions.

These previous works simply focus on the performance of wireless communications without considering adaptive discrete modulation and energy harvesting. These techniques, in fact, was studied separately in [17]–[24]. More precisely, authors in [17] investigated performance of the CRNs with EH relay assistance. They showed that their proposed EH relaying outperforms the conventional underlay CRN scheme in the OP. Thanh and others investigated the performance of the SWIPT-enabled networks [18], [19]. They proved that low energy devices can be operated without a battery provided that the number of transmit antennae at BS goes to infinity. The cooperative NOMA-based with SWIPT over Nakagami- $m$  fading channels was addressed in [20]. The self-energy recycling (SER) scheme was studied in [21] under partial and full relay selection. To be more specific, they proposed to utilize the self-interference at the full-duplex relay to recharge its battery and forward information to the destination. Besides, Tung in [20] studied the combination of SWIPT and NOMA over Nakagami- $m$  channels. The potential of the application of mmWave combined with SWIPT was thoroughly studied in [22]. Meanwhile, the adaptive multicast streaming service with ADM in cellular networks was addressed in [23] and the average and potential throughput of the adaptive modulation was derived in [24].

### B. Principal novelties and contributions

Apart from works in the literature, we comprehensively investigate the performance of the mobile networks with the combination of adaptive discrete modulation and energy harvesting at the system level. More precisely, we summarize the core novelties and contributions as follows:

- We consider the Poisson point process (PPP) to model the randomness of mobile users (MUs) and base stations (BSs).
- We employ the power beacon scheme to charge the battery of MUs instead of using the SWIPT protocol and the bounded path-loss model is used as well.
- We adopt adaptive modulation to take the benefits of the channel state information (CSI) at MUs.

- Compared with state-of-the-art, we consider the spatial-temporal correlation at the signal-to-interference-plus-noise ratios (SINRs) which is extremely complicated and nontrivial.
- We investigate the performance of three key metrics i.e., achievable spectral efficiency, occurrence probabilities of modulation schemes, and coverage probability.
- Numerical results based on the Monte Carlo method is yield highlight the advantages of the considered networks compared with a fixed modulation scheme.

## II. SYSTEM MODEL

### A. Cellular Networks Modeling

Considering a uplink cellular networks that both base stations and mobile users are followed by a homogeneous PPP (HPPP) denoted by  $\Xi_{BS}$  and  $\Xi_{MU}$  with corresponding densities  $v_{BS}$  and  $v_{MU}$ . Additionally, without loss of generality, we consider the fully-loaded scenario, i.e.,  $v_{MU} \gg v_{BS}$ . It is noted that the most general case where the ratio of the density of BSs and MUs is a random number is studied in [25]. The performance is taken place at the typical cell where the serving BS denoted by  $BS_0$  and the typical user denoted by  $MU_0$  is situated at the origin of the 2-D plane. The results measure the link between  $BS_0$  and  $MU_0$  can be applied to all other transmission link thank to the Palm theory [26].

### B. Transmission Procedure

The whole transmission is taken place in two phases. In the first phase, the  $BS_0$  broadcasts high-power radio frequency signals to charge the battery of all MUs associated with it. In the second phase, the  $MU_0$  which is selected to send data to the  $BS_0$ <sup>1</sup> using the energy harvesting in the first phase as well as on the instantaneous channel state information which is measured via the pilot signals in the first phase. It is emphasized that we do not consider the simultaneous information and power transmission since it scarifies parts of resources (time or frequency) for powering the battery. Moreover, the BS acts as the power beacon station both two phases. We consider the orthogonal resource allocation inside each cell. Hence, intra-interference in each cell is not taken into consideration, nonetheless, other-cell interference, obviously, is appeared.

### C. Channel Modelling

Considering an arbitrary connection from a generic BS to a generic MU, it experiences small-scale fading and large-scale path loss. Shadowing is left for future work like work in the literature [27].

1) *Small-scale fading*: Considering  $c_m$  as the small-scale fading for a transmission between the BSs and MUs followed by a Rayleigh distribution. As a consequence,  $|c_m|^2$  is an exponential distribution have mean  $\lambda_m = 1, \forall m$  (w ithout loss of generality) denoting the channel gain.

<sup>1</sup>In the present paper, we do not focus on the user selection and leave it for future work.

2) *Large-scale path-loss*: The large-scale path-loss of an arbitrary link between BSs and MUs is evaluated as

$$W_m = W_0 \max\{d_m, 1\}^\alpha. \quad (1)$$

Here  $d_m$  is the transmission distance between BSs and MUs;  $\alpha > 2$  and  $W_0 = (4\pi f_c/c)^2$  are the path-loss and exponent.  $f_c$  (in Hz) denotes carrier frequency,  $c = 3 \times 10^8$  (in meters per second) is the light speed.

*Remark 1*: Direct inspection (1), we can see that the adopted large-scale path-loss overcomes the unavoidable issue of the popular unbounded path-loss model that the received power approaches infinity when the transmission distance between indistinguishable [28].

#### D. Cell Association Criterion

Each MU is handled by a BS having the shortest distance to it. As the fully-loaded scenario is considered, all BSs are active. The serving BS,  $BS_0$ , is then formulated as

$$BS_0 = \operatorname{argmin}_{m \in \Xi_{BS}} \{W_m\}. \quad (2)$$

#### E. Adaptive Discrete Modulation

Adaptive discrete modulation is a mature technology to boost spectral efficiency especially when the channel is favorable. Particularly, based on the pilot signals at the first phase, the  $MU_0$  exactly estimates the CSI between him and  $BS_0$ . Moreover, since we consider the fully-loaded scenario that is the worst case where all BSs are active, the MUs are then estimated at the interference at the  $BS_0$ . Based on the available CSI, the  $MU_0$ , then, selects the most appropriate modulation scheme that satisfies the quality-of-service (QoS) requirement. Let us first divide the whole range of SINR at  $BS_0$  into  $\mathcal{R} \in \mathbb{N}$  separate regions and the border of each interval is denoted by  $\gamma_R^e$ ,  $e \in \{0, \dots, \mathcal{R}\}$ , as follows:

$$0 = \gamma_R^0 < \gamma_R^1 < \dots < \gamma_R^e < \dots < \gamma_R^{\mathcal{R}} = +\infty \quad (3)$$

The popular rectangular  $M$ -QAM modulation is adopted in the present paper. More precisely,  $M_o = 2^o$ -QAM modulation is chosen provided that the SINR lies into the interval  $[\gamma_R^o, \gamma_R^{o+1})$ ,  $o \in \{1, \dots, \mathcal{R} - 1\}$ . Additionally, in case the SINR is too small or it is in the region  $[\gamma_R^0, \gamma_R^1)$ ,  $MU_0$  will immediately halt the transmission and the outage event will appear.

In order to find out the border of all regions, we examine bit error rate (BER) as a measured metric. Particularly, BER of the  $M$ -QAM employing Gray coding over additive white Gaussian channel (AWGN) is deployed:

$$\begin{aligned} \text{BER}_R &= \beta_o Q(\sqrt{\chi_o \gamma_R^o}) \\ \Rightarrow \gamma_R^o &= \frac{1}{\chi_o} \left[ Q^{-1} \left( \frac{\text{BER}_R}{\beta_o} \right) \right]^2, \quad o \in \{1, \dots, \mathcal{R} - 1\}, \end{aligned} \quad (4)$$

where  $\text{BER}_R$  is the intended bit error rate threshold;  $Q(\cdot)$  is the Gaussian Q function and  $Q^{-1}(\cdot)$  is the inverse Gaussian

Q function.

$$\begin{aligned} \beta_o &= \begin{cases} 1 & l_o = 1, 2 \\ 4/l_o & l_o \geq 3 \end{cases}, \\ \chi_o &= \begin{cases} 2/l_o & l_o = 1, 2 \\ 3/(2^{l_o} - 1) & l_o \geq 3 \end{cases} \end{aligned} \quad (5)$$

where  $l_o = \log_2(M_o)$ .

#### F. Transmit Power at MUs

In this work, the harvest-then-transmit protocol is employed at the MUs that harvested energy amount in the first phase denoted by  $\mathcal{E}$  (in Joule) is computed as follows:

$$\mathcal{E} = \epsilon T \left( P_{\text{tx}} \sum_{i \in \Xi_{BS}} \frac{|c^{(i)}|^2}{W^{(i)}} \right) / 2. \quad (6)$$

Here  $\epsilon \in [0, 1]$  denote the coefficient of energy conversion;  $T$  is the whole transmission block and is equal to 1 for simplicity;  $P_{\text{tx}}$  is the BSs transmit power. It should be noted that the AWGN noise in (6) is ignored since it is too tiny compared to power of interference. From (6), the MUs transmit power is computed as follows:

$$P_0 = \frac{\epsilon}{2} \left( P_{\text{tx}} \sum_{i \in \Xi_{BS}} \frac{|c^{(i)}|^2}{W^{(i)}} \right). \quad (7)$$

#### G. Signal-to-Interference-Plus-Noise Ratio

The SINR at  $BS_0$  is given as

$$\gamma_0 = \frac{P_0 \frac{|c^{(0)}|^2}{W^{(0)}}}{P_{\text{MU}} \sum_{j \in \Xi_{\text{MU}}} \frac{|c^{(j)}|^2}{W^{(j)}} + \sigma_0^2}, \quad (8)$$

where  $\sigma_0^2 = -174 + \text{NF} + 10 \log_{10}(\text{BW})$  (in dBm) is the  $BS_0$  noise variance;  $\text{NF}$  (in [dB]) is the noise figure at the ED;  $\text{BW}$  is the bandwidth;  $P_{\text{MU}} = \mathbb{E}\{P_0\}$  is the transmit power of the MUs from other cell. In this work, for simplicity, we assume that  $P_{\text{MU}}$  is the average over spatial (MUs locations) and temporal (fading) of the whole networks. The spatial-temporary correlation at the transmit power of the MUs will be left for future work.  $\mathbb{E}\{\cdot\}$  is the expectation operator.  $c^{(s)}$ ,  $W^{(s)}$ ,  $s \in \{0, j\}$ , are the path-loss and fading between the  $BS_s$  and  $MU_0$ .

*Remark 2*: Inspecting (8), we observe that although the spatial-temporary correlation at  $P_{\text{MU}}$  do not take into consideration, these correlations at  $P_0$  still hold. As a consequence, the considered networks are extremely complicated and novel compared with work in the literature [29].

### III. PERFORMANCE METRICS

We investigate three key metrics in the present work, i.e., the average achievable spectral efficiency, the coverage probability, and the occurrence probabilities of different modulation schemes (Poc). More precisely, Pcov is the probability that measures the number of outstanding transmissions out of the total transmission while Poc measures the percentage of each

TABLE I: Simulation parameters

Parameters [Unit]	Values
$R_{BS} = \frac{1}{\sqrt{\pi v_{BS}}} [m]$	150
$R_{MU} = \frac{1}{\sqrt{\pi v_{MU}}} [m]$	50
$P_{tx} [dBm]$	30
$BER_R$	$10^{-3}$
$BW [kHz]$	200
$\epsilon$	0.5
$\mathcal{R}$	5
$NF [dB]$	5
$\alpha$	2.3
$f_c [GHz]$	0.9

scheme appearance out of all transmissions. The ASE provides the average achievable spectral efficiency.

#### A. Coverage Probability

The Pcov under the considered network refers to the probability that the SINR of the BS<sub>0</sub> is larger than  $\gamma_R^1$  and is computed as

$$P_{cov} = \Pr \{ \gamma_{\Delta} \geq \gamma_R^1 \}. \quad (9)$$

#### B. Occurrence probabilities of each modulation scheme

The probability that the MU<sub>0</sub> transmits at  $o$  modulation scheme defines as the occurrence probabilities denoted by  $\Psi_o$  and is computed as

$$\Psi_o = \Pr \{ \gamma_R^o \leq \gamma_0 \leq \gamma_R^{o+1} \}, \quad o \in \{1, \dots, \mathcal{R} - 1\}. \quad (10)$$

It is obvious that the summation of  $\Psi_o$ ,  $o \in \{0, \dots, \mathcal{R} - 1\}$  is equal to one. In particular, we have

$$\sum_{o=0}^{\mathcal{R}-1} \Psi_o = 1. \quad (11)$$

#### C. Average Achievable Spectral Efficiency (ASE)

Under the adaptive modulation systems, the average achievable spectral efficiency (in bits/s/Hz) is computed by summing all the spectral efficiency of each region that is the multiplication of the P<sub>oc</sub> and its corresponding bit and is given as follows [6]:

$$ASE = \sum_{o=1}^{\mathcal{R}-1} l_o \Psi_o. \quad (12)$$

### IV. NUMERICAL RESULTS

Numerical results via the Monte-Carlo simulation are employed in this section to evaluate the performance of the considered metrics, i.e., Pcov, P<sub>oc</sub>, and ASE. If there is no specific noticed in each figure, a set of simulation parameters is given in Table I. Here,  $R_{BS}$  and  $R_{MU}$  are the average cell radius of the BS and the average distance between MUs, respectively. Five levels of the  $M$ -QAM modulation are considered [6], specifically, no transmission, BPSK, QPSK, 16-QAM, and 64-QAM, respectively. It is certain that an arbitrary modulation level and/or different modulation schemes such as

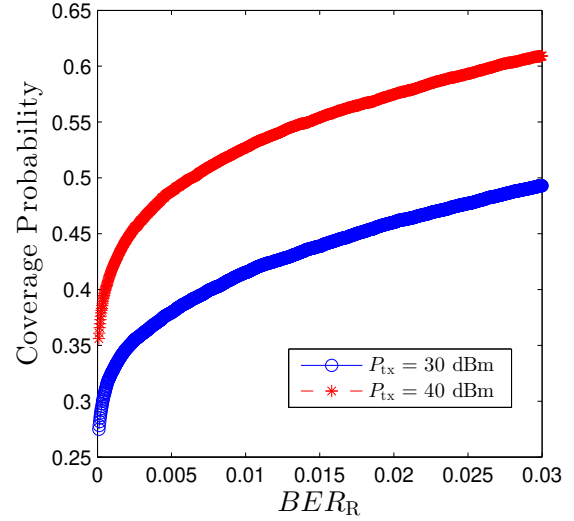


Fig. 1. Pcov as a function of BER threshold,  $BER_R$  with various values of  $P_{tx}$ .

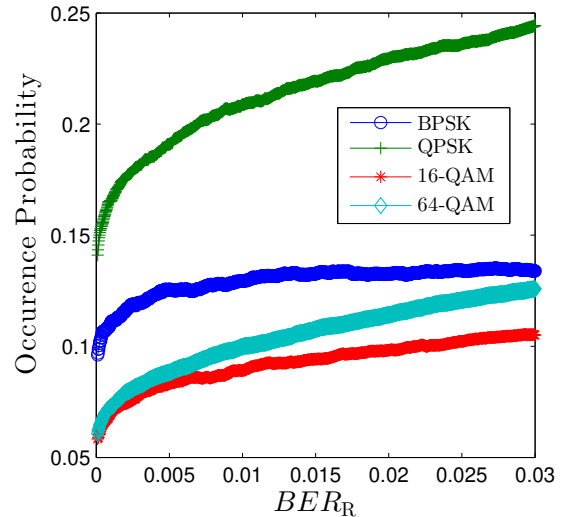


Fig. 2. Occurrence probability vs. BER threshold,  $BER_R$ .

MPSK, differential modulation, etc. can also be effortlessly applied. Fig. 1 depicts the behaviors of the Pcov regarding the BER threshold. We observe that if the QoS decreases, the Pcov improves, and increasing  $P_{tx}$  is beneficial for the Pcov. Particularly, Pcov enhances over 0.1 if  $P_{tx}$  increases from 30 to 40 dBm at  $BER_R = 0.01$ .

Fig. 2 shows the behaviors of the occurrence probability as a function of  $BER_R$ . We see that under the current setup, the QPSK has the highest probability while the 16-QAM is the smallest one, and BPSK and 64-QAM are at the 2nd and 3rd position. Again, increasing  $BER_R$  will scale up the P<sub>oc</sub> like the Pcov. However, the increasing pace is different between these schemes. More precisely, the QPSK is again

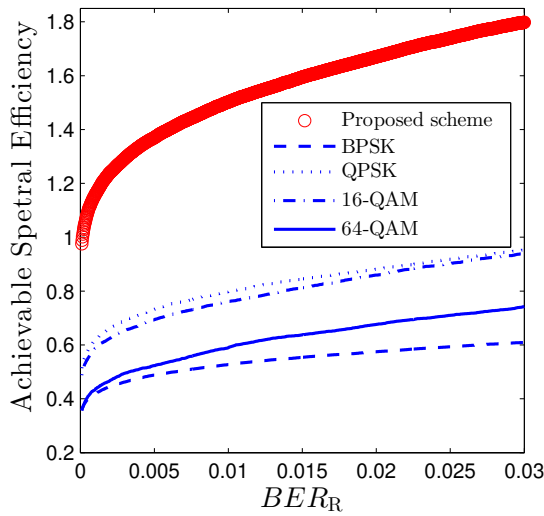


Fig. 3. ASE vs. BER threshold,  $BER_R$ .

favorable for the increase of  $BER_R$  while the BPSK is almost stable when  $BER_R \geq 0.01$ . The performance of the ASE with respect to  $BER_R$  is given in Fig. 3. It proves the superiority of the ADM compared with the fixed modulation. Particularly, we experience a major divergence between the proposed scheme vs. all other modulations. Among all fixed modulations, the QPSK achieves the best performance as like in Fig. 2. Nonetheless, different from Fig. 2, the 16-QAM is the 2nd best while in Fig. 2, the 2nd best is the BPSK modulation.

## V. CONCLUSION

The performance of uplink cellular networks considering both adaptive modulation and energy harvesting was investigated in the present paper. Particularly, three vital metrics, i.e., Pcov, Poc, and ASE are addressed under the impact of both spatial and temporary correlation. Simulation results unveiled that adaptive modulation significantly outperforms fixed modulation schemes in terms of spectral efficiency. This work can be enhanced in many ways. One of these possible ways is to deploy diversity techniques at the BSs and/or MUs to further enhance the Pcov and ASE [30]. Additionally, the application of reconfigurable intelligent surfaces (RIS) and NOMA into the ultra-dense cellular networks is also promising [31]–[33]. The heterogeneous networks architecture where cellular networks co-exist with other networks such as cognitive radio networks, low power wide area networks (LoRa, Sig-Fox), and device-to-device communications also scales up the system spectral efficiency [34], [35]. Facilitating the system performance by shortening the transmission distance such as multi-hop communications, and cooperative communications is a potential solution too. Finally, the advantages of machine learning and deep learning can not be ignored in order to significantly enhance the system performance as well [36], [37].

## REFERENCES

- [1] Ericsson Mobility Report, Ericsson, 2017.
- [2] N. Q. Sang *et al.*, "Cognitive multihop cluster-based transmission under interference constraint," *2014 IEEE ISCE*, 2014, pp. 1-3.
- [3] L. -T. Tu *et al.*, "Performance Evaluation of Incremental Relaying in Underlay Cognitive Radio Networks with Imperfect CSI," *2020 IEEE ICCE*, 2021, pp. 472-477.
- [4] T. N. Nguyen *et al.*, "Outage Performance of Satellite Terrestrial Full-Duplex Relaying Networks with Co-Channel Interference," *IEEE Wireless Commun. Lett.*, vol. 11, no. 7, pp. 1478-1482.
- [5] J. Song *et al.*, "On the feasibility of interference alignment in ultra-dense millimeter-wave cellular networks," *IEEE Asilomar 2016*, 2016, pp. 1176-1180.
- [6] M. S. Alouini *et al.*, "Adaptive modulation over nakagami fading channels," *Wireless Pers. Commun.*, vol. 13, pp. 119-143, May. 2000.
- [7] J. Huang, C.-C. Xing, and C. Wang, "Simultaneous wireless information and power transfer: Technologies, applications, and research challenges," *IEEE Commun. Magazine*, vol. 55, pp. 26-32, Nov. 2017.
- [8] P. N. Son *et al.*, "Short packet communications for cooperative UAV-NOMA-based IoT systems with SIC imperfections," *Compt. Netw.*, 2022.
- [9] L.-T. Tu *et al.*, "A New Closed-Form Expression of the Coverage Probability for Different QoS in LoRa Networks," *IEE ICC 2020*.
- [10] J. G. Andrews *et al.*, "A Tractable Approach to Coverage and Rate in Cellular Networks," *IEEE Trans. Commun.*, vol. 59, no. 11, 2011.
- [11] T. L. Thanh *et al.*, "Capacity analysis of multi-hop decode-and-forward over Rician fading channels," *IEEE ComManTel 2014*, 2014, pp. 134-139.
- [12] T. T. Duy *et al.*, "Performance Enhancement for Multihop Cognitive DF and AF Relaying Protocols under Joint Impact of Interference and Hardware Noises: NOMA for Primary Network and Best-Path Selection for Secondary Network," *Wireless Commun. Mobile Comput.*, vol. 2021.
- [13] L. -T. Tu *et al.*, "Broadcasting in Cognitive Radio Networks: A Fountain Codes Approach," *IEEE Trans. Veh. Technol., Early Access*, 2022.
- [14] T. L. Thanh *et al.*, "10-Gb/s wireless signal transmission over a seamless IM/DD fiber-MMW system at 92.5 GHz," *IEEE ICC 2015*, 2015, pp. 1364-1369.
- [15] C. H. Duc *et al.*, "Performance Evaluation of UAV-Based NOMA Networks with Hardware Impairment," *Electronics*, vol. 11, no. 1, p. 94, Dec. 2021.
- [16] T. T. Lam *et al.*, "On the Spectral Efficiency of LoRa Networks: Performance Analysis, Trends and Optimal Points of Operation," *IEEE Trans. Commun.*, vol. 70, no. 4, pp. 2788-2804, April 2022.
- [17] P. N. Son *et al.*, "Performance analysis of underlay cooperative cognitive full-duplex networks with energy-harvesting relay," *Compt. Netw.*, vol. 122, p. 9-19, Jun. 2018.
- [18] L.-T. Tu *et al.*, "System-level analysis of swipt mimo cellular networks," *IEEE Commun. Lett.*, vol. 20, pp. 2011-2014, Oct. 2016.
- [19] L.-T. Tu *et al.*, "System-level analysis of receiver diversity in swipt-enabled cellular networks," *IEEE/KICS J. Commun. Netw.*, vol. 18, pp. 926-937, Dec. 2016.
- [20] T.-T. Nguyen *et al.*, "Evaluation of Full-Duplex SWIPT Cooperative NOMA-Based IoT Relay Networks over Nakagami-m Fading Channels," *Sensors*, vol. 22, no. 5, p. 1974, Mar. 2022.
- [21] T. N. Nguyen *et al.*, "Partial and Full Relay Selection Algorithms for AF Multi-Relay Full-Duplex Networks With Self-Energy Recycling in Non-Identically Distributed Fading Channels," *IEEE Trans. Veh. Technol.*, vol. 71, no. 6, pp. 6173-6188, Jun. 2022.
- [22] T. T. Lam *et al.*, "Analysis of millimeter wave cellular networks with simultaneous wireless information and power transfer," *IEEE SigTelCom 2017*, 2017, pp. 39-43.
- [23] M. Li *et al.*, "Performance analysis of adaptive multicast streaming services in wireless cellular networks," *IEEE Trans. Mobile Comput.*, vol. 18, pp. 2616-2630, Nov. 2019.
- [24] X. Qiu *et al.*, "On the performance of adaptive modulation in cellular systems," *IEEE Trans. Commun.*, vol. 47, pp. 884-895, Jun. 1999.
- [25] T. T. Lam *et al.*, "On the Energy Efficiency of Heterogeneous Cellular Networks With Renewable Energy Sources—A Stochastic Geometry Framework," *IEEE Trans. Wireless Commun.*, 2020.
- [26] F. Baccelli and B. Błaszczyszyn, *Stochastic Geometry and Wireless Networks, Part I: Theory*, Now Publishers, Sep. 2009.

- [27] M. Di Renzo *et al.*, "System-Level Modeling and Optimization of the Energy Efficiency in Cellular Networks – A Stochastic Geometry Framework", *IEEE Trans. Wireless Commun.*, vol. 17, no. 4, pp. 2539 - 2556, Apr. 2018.
- [28] J. Song *et al.*, "Bounded Path-Loss Model for UAV-to-UAV Communications," *ICWMC 2021*, pp. 20-21.
- [29] H. H. Yang *et al.*, "Spatio-Temporal Analysis for SINR Coverage in Small Cell Networks," *IEEE Trans. Commun.*, vol. 67, no. 8, pp. 5520-5531, Aug. 2019.
- [30] P. T. Tin *et al.*, "Rateless Codes-Based Secure Communication Employing Transmit Antenna Selection and Harvest-To-Jam under Joint Effect of Interference and Hardware Impairments," *Entropy*, vol. 21, no. 7, p. 700, Jul. 2019.
- [31] T. -T. T. Dao *et al.*, "Performance Evaluation of Downlink Multiple Users NOMA-Enable UAV-Aided Communication Systems Over Nakagami-m Fading Environments," *IEEE Access*, vol. 9, pp. 151641-151653, 2021.
- [32] T. V. Chien *et al.*, "Coverage Probability and Ergodic Capacity of Intelligent Reflecting Surface-Enhanced Communication Systems," *IEEE Commun. Lett.*, vol. 25, no. 1, pp. 69-73, Jan. 2021.
- [33] T. V. Chien *et al.*, "Outage Probability Analysis of IRS-Assisted Systems Under Spatially Correlated Channels," *IEEE Wireless Commun. Lett.*, vol. 10, no. 8, pp. 1815-1819, Aug. 2021.
- [34] L. -T. Tu *et al.*, "Energy Efficiency Analysis of LoRa Networks," *IEEE Wireless Commun. Lett.*, vol. 10, no. 9, pp. 1881-1885, Sept. 2021
- [35] L. -T. Tu *et al.*, "Coverage Probability and Spectral Efficiency Analysis of Multi-Gateway Downlink LoRa Networks," *IEEE ICC 2022* 2022, pp. 1-6.
- [36] L. -T. Tu *et al.*, "Energy Efficiency Optimization in LoRa Networks—A Deep Learning Approach," *IEEE Trans. Intel. Transport. Syst., Early Access*, 2022.
- [37] A. Zappone *et al.*, "Model-aided wireless artificial intelligence: Embedding expert knowledge in deep neural networks for wireless system optimization," *IEEE Veh. Technol. Mag.*, vol. 14, pp. 60–69, Sep. 2019.